DOI: 10.1002/chem.200903073

Unravelling the Reaction Mechanism for the Fast Photocyclisation of 2-Benzoylpyridine in Aqueous Solvent by Time-Resolved Spectroscopy and Density Functional Theory Calculations

Yong Du,[a, b] Jiadan Xue,[a, c] Ming-De Li,[a] Xiangguo Guan,[a] David W. McCamant,[b] and David Lee Phillips*[a]

Abstract: A combined femtosecond transient absorption (fs-TA) and nanosecond time-resolved resonance Raman (ns-TR^3) spectroscopic investigation of the photoreaction of 2-benzoylpyridine (2-BPy) in acetonitrile and neutral, basic and acidic aqueous solvents is reported. fs-TA results showed that the nπ^* triplet 2-BPy is the precursor of the photocyclisation reaction in neutral and basic aqueous solvents. The *cis* triplet biradical and the *cis* singlet zwitterionic species produced during the photocyclisation reaction were initially characterised by ns-TR^3 spectroscopy. In addition, a new species was uniquely observed in basic aqueous solvent after the decay of the *cis* singlet zwitterionic species and this new species was tentatively assigned to the photocyclised radical anion. The ground-state conformation of 2-BPy in acidic aqueous solvent is the pyridine nitrogen-protonated 2-BPy cation (2-BPy-NH$^+$) rather than the neutral form of 2-BPy. After laser photolysis, the singlet excited state (S_1) of 2-BPy-NH$^+$ is generated and evolves through excited-state proton transfer (ESPT) and efficient intersystem crossing (ISC) processes to the triplet exited state (T_1) of the carbonyl oxygen-protonated 2-BPy cation (2-BPy-OH$^+$) and then photocyclises with the lone pair of the nitrogen atom in the heterocyclic ring. Cyclisation reactions take place both in neutral/basic and acidic aqueous solvents, but the photocyclisation mechanisms in these different aqueous solvents are very different. This is likely due to the different conformation of the precursor and the influence of hydrogen-bonding of the solvent on the reactions.

Keywords: cyclization · photochemistry · Raman spectroscopy · reaction mechanisms · solvent effects · time-resolved spectroscopy

Introduction

The photochemistry and photophysics of benzophenone (BP) and of its derivatives have been the subjects of many studies due to their importance in understanding the photosensitiser mechanisms of electron transfer and hydrogen abstraction in the lowest triplet electronic excited states.[1–32] Di(*n*-pyridyl) ketones (*n*-DPK)[3,7–9,12,29,32,35] and *n*-benzoylpyridines (*n*-BPy)[4–6,13–16,20,29,31–32,35–36] (*n* represents the position of the nitrogen atom position within the aromatic rings) are particularly interesting because they contain heteroaromatic ring(s) in which the nitrogen atom may appear at different positions within the molecule and this can significantly change the photophysical properties and photochemical reactivity of their nπ^* triplet states.[6,8,13,15,16,18] The lifetimes of the triplet states of *n*-DPK and *n*-BPy with $n=3$ and 4 are shorter than that of BP due to the electron-withdrawing effect of the heterocyclic nitrogen atom,[5,6,8,13–15] but they still undergo hydrogen abstraction reactions similar to BP[13,15,36] and form ketyl radical analogue intermediates that produce a light-absorbing transient (LAT) in hydrogen-donor solvents such as 2-propanal.[31]

However, 2-DPK and 2-BPy display appreciably different photodegradation behaviour in solvents with hydrogen-

[a] Y. Du, J. Xue, M.-D. Li, X. Guan, D. L. Phillips
Department of Chemistry, The University of Hong Kong
Pokfulam Road, Hong Kong (P.R. China)
Fax: (+852) 2857-1586
E-mail: phillips@hkucc.hku.hk

[b] Y. Du, D. W. McCamant
Department of Chemistry, The University of Rochester
Rochester, New York 14627 (USA)

[c] J. Xue
Current address: Department of Chemistry
The Ohio State University
100 West 18th Ave., Columbus, Ohio 43210 (USA)

Supporting information for this article is available on the WWW under http://dx.doi.org/10.1002/chem.200903073.

bonding ability because intramolecular cyclisation reactions take place. Scheme 1 shows the proposed photocyclisation reaction pathways of 2-BPy in aqueous solvent as proposed by Hurt and Filipescu[4] as well as by Favaro and co-workers.[16,20] By irradiation of **1** in a degassed aqueous solution, Hurt and Filipescu[4] observed orange **3′**, which was identified by characterisation of air-sensitive hydrochloride **13'**, formed in the presence of dry HCl in degassed tetrahydrofuran, and a yellow-orange solid **12'**, formed by sodium reduction in EtOH. Favaro and co-workers[16,20] suggested the prevailing reaction pathway should involve an attack of the carbon atom in the pyridyl group because they identified product **10** by monitoring the changes in the product's UV absorption spectrum after acidification and basification of the solution. In addition, Favaro and co-workers detected two transient species by a time-resolved absorption technique. One of these two short-lived intermediates with $\lambda_{max}=475$ nm and $\tau=450$ ns in water was assigned to diradical **2** and the other with $\tau=600$ μs in water was identified as having the zwitterionic structure **3**. At room temperature, the zwitterions **3** produced species **8**, which decayed in hours by thermal loss of a hydrogen atom to **9**, which was transformed into **10** in the presence of air.[20]

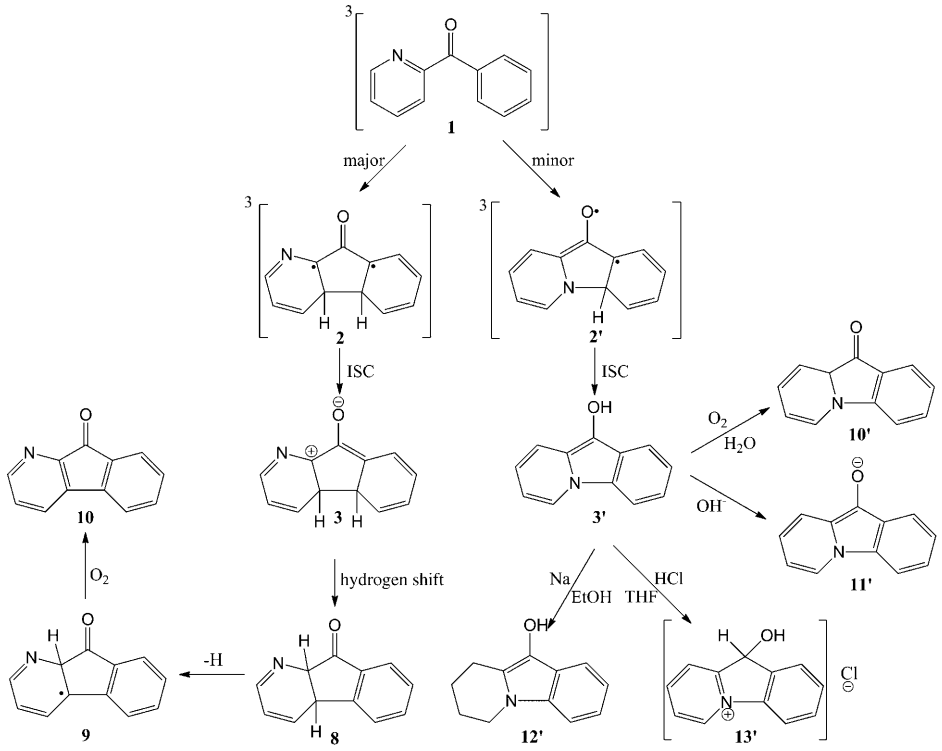

Scheme 1. Photocyclisation reaction pathways of 2-BPy in aqueous solvents proposed by Hurt and Filipescu[4] and Favaro and co-workers.[16]

The properties of *n*-BPy in acidic aqueous solutions have also attracted attention. It was found that the lifetimes of *n*-BPy are shorter in acidic aqueous solution than BP, but the reason for this is not clear.[5,6] Moreover we note that there are few studies on the early behaviour of 2-BPy, especially in aqueous solvent.[16,20] Clear characterisation of the kinetics and other properties of the transient species by laser flash photolysis (LFP) is hampered because of the featureless overlapping of the absorption bands of these species and their coexistence on the same timescale.

In this work femtosecond transient absorption (fs-TA) and nanosecond time-resolved resonance Raman (ns-TR^3) experiments were performed on 2-BPy in acetonitrile (MeCN), H_2O/MeCN (1:1 by volume) and H_2O/MeCN containing 0.05 M NaOH and $HClO_4$ (denoted hereafter as neutral, basic and acidic aqueous solvents, respectively). To the best of our knowledge, this is the first study of the overall direct vibrational and structural characterisation of the intermediates and dynamics of the photocyclisation reaction mechanism(s) of the photoreaction of 2-BPy in aqueous solvents following UV laser photolysis. ns-TR^3 spectroscopy is an effective technique for more clearly characterising the structural and electronic properties of transient species and has been used to help identify the intermediates and photoproducts of BP, 3-BPy and 4-BPy in 2-propanal and aqueous solvents.[28,31,36,37] To help determine the geometries of these intermediate species and to assign the experimental vibrational bands, density functional theory (DFT) calculations were performed by using the (U)B3LYP methods with the 6-311G** basis set for all of the species examined herein. These results have provided us with useful information about the photoreaction of 2-BPy and generated firm evidence for the reaction mechanism(s) of this molecule in aqueous solvents under different pH conditions. The fs-TA and ns-TR^3 measurements indicated that the lowest triplet state of 2-BPy has an $n\pi^*$ configuration and is the precursor of the photocyclisation reaction in neutral/basic aqueous solvents. In neutral/basic aqueous solvents, two short-lived intermediates **2** and **3** were identified and characterised by resonance Raman spectra, which supported previous tentative assignments made on the basis of LFP.[16] In acidic aqueous solvent, as a result of a different precursor conformation and the effect of hydrogen-bonding with the solvent, 2-BPy exhibits a distinctly different reaction pathway. This paper presents the first characterisation of the photochemical reactions of 2-BPy in acidic aqueous solvent on the femto- to

microsecond timescale. In acidic aqueous solvent, the singlet excited state (S_1) of the pyridine nitrogen-protonated 2-BPy cation (2-BPy-NH^+) is generated from the ground state (S_0) of 2-BPy-NH^+ after laser photolysis and then evolves into the triplet exited state (T_1) of the carbonyl oxygen-protonated 2-BPy cation (2-BPy-OH^+). 2-BPy-OH^+ then photocyclises with the nitrogen lone-pair involved in the cyclisation process. Although cyclisation reactions take place in both neutral/basic and acidic aqueous solvents, the reaction mechanisms in these two different types of aqueous solvents are very different to one another.

Results and Discussion

Steady-state UV/Vis spectra: Figure 1 shows the UV/Vis spectra of 2-BPy recorded in neat MeCN and neutral, basic and acidic aqueous solvents. It can be seen that the absorption spectrum of 2-BPy in MeCN has a strong band with a maximum at 260 nm characteristic of a $\pi\pi^*$ absorbance transition and is very similar to the absorption spectrum of the parent BP.[11] In neutral and basic aqueous solvents, the full-width at half-maximum (FWHM) of this absorption band remains unchanged and the absorption band is redshifted relative to the band in neat MeCN. The formation of hydrogen bonds with the aqueous solvent accounts for these small redshifts, and thus in neutral and basic aqueous solvents the ground state 2-BPy should have the same neutral form as that in MeCN. However, in acidic solvents containing 0.03 and 0.05 M $HClO_4$, in addition to the redshift of the absorption band relative to that in the neutral aqueous solvent, the FWHM of the band becomes much narrower and this is likely due not just to the influence of the hydrogen-bonding solvent effect. Increasing the concentration of acid in the solvent leads to the formation of a new band at $\approx$300 nm. In an acidic solvent containing 12 M $HClO_4$, the band at 300 nm is clear and strong. The new band at 300 nm is substantially different to that at $\approx$340 nm arising from the carbonyl oxygen-protonated BP cation (BP-OH^+).[24,30,34] On the basis that the pyridine nitrogen atom is easily protonated and that carbonyl oxygen protonation of the ground state BP is negligible in 5.8 M $HClO_4$,[34] it is probable that in acidic aqueous solvents containing 0.03 and 0.05 M $HClO_4$, 2-BPy-NH^+ coexists with the neutral form of 2-BPy.

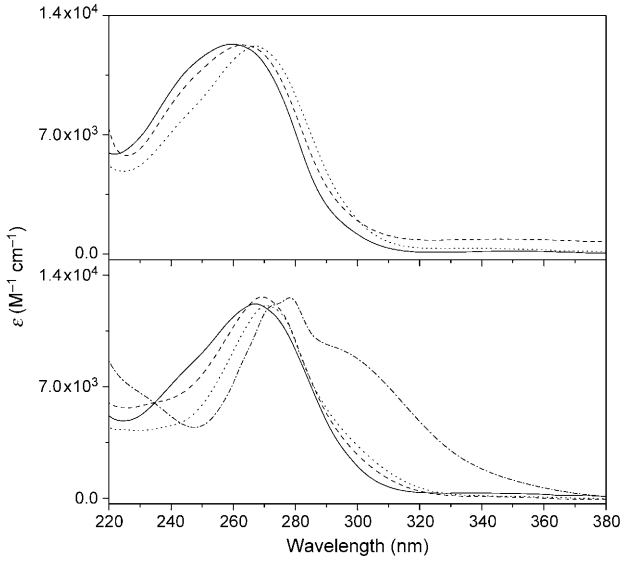

Figure 1. Top) UV/Vis spectra of 2-BPy in neat MeCN (solid), neutral (dot) and basic (dash) aqueous solvents. Bottom) UV/Vis spectra of 2-BPy in neutral aqueous solvent (solid) and in acidic aqueous solvents containing 0.03 (dash line), 0.05 (dot) and 12 M (dash dot) $HClO_4$.

Resonance Raman (RR) spectroscopy: The RR spectra obtained on 309.1 nm excitation of 2-BPy in MeCN and neutral, basic and acidic aqueous (containing 0.05 M NaOH and $HClO_4$) solvents and a comparison of these spectra with the DFT-calculated normal Raman spectra of the ground-state 2-BPy-NH^+ are displayed in Figure 2. Examination of Figure 2 shows that the RR spectra of 2-BPy observed in neutral and basic aqueous solvents are essentially identical with the same intensity and frequency distributions, but slightly different to that observed in MeCN (see the two bands between 1400 and 1500 cm^{-1}). The different relative intensities of the Raman bands at 1545 and 1584 cm^{-1}, which correspond to aromatic stretching of the pyridyl and phenyl groups, respectively, can be attributed to hydrogen-bonding at the pyridine nitrogen atom in aqueous solvents and the accompanying changes in the geometry of 2-BPy. In addition, the hydrogen-bonding effect at the carbonyl

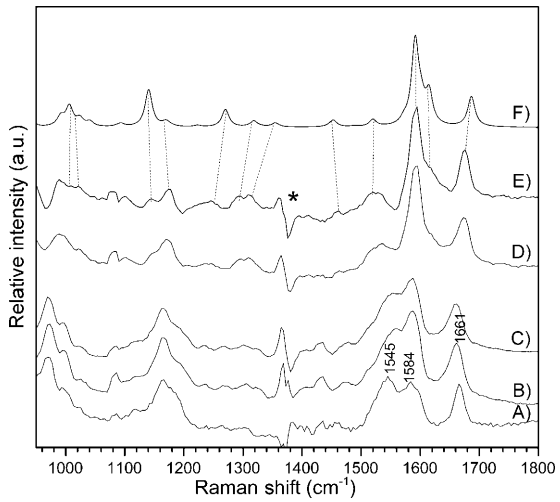

Figure 2. The RR spectra of 2-BPy in A) neat MeCN, B) neutral, C) basic and D) acidic aqueous solvents obtained on 309.1 nm excitation. E) The difference spectrum obtained by subtraction of the RR spectrum recorded in neutral solvent from the RR spectrum in acidic solvent. F) DFT-calculated Raman spectrum for the ground state 2-BPy-NH^+. The asterisk marks a region affected by solvent subtraction artefacts.

oxygen atom is also evident in the RR spectra. For example, the Raman feature at 1665 cm^{-1} in neat MeCN corresponding to the C=O stretching vibrational mode shows a 4 cm^{-1} frequency upshift compared with those at 1661 cm^{-1} recorded in neutral and basic aqueous solutions. This result is in agreement with the expected hydrogen-bonding interaction at the carbonyl oxygen atom lengthening the C=O bond and weakening its restoring force leading to a downshift of its vibrational frequency.

In the acidic aqueous solvent, the RR spectrum for 2-BPy is significantly different to that recorded in the neutral aqueous solvent. This is visible not only in the frequencies but also in the relative intensities of the vibrational modes, especially for the three Raman bands in the 1400–1500 cm^{-1} region. The contribution of the neutral form of 2-BPy was removed by subtracting an appropriately scaled Raman spectrum recorded in neutral aqueous solvent so that the strongest Raman band at 1584 cm^{-1} for the neutral form 2-BPy was completely removed. The difference spectrum is presented in Figure 2E and it can be seen that it is very similar to the unsubtracted spectrum recorded in acidic solvent. This indicates that the neutral form of 2-BPy exists as a "minor" contribution in the acidic solvent. A computed Raman spectrum for 2-BPy-NH^+ is presented in Figure 2F and allows a comparison with the difference Raman spectrum. The calculated frequencies and the tentative assignments of the experimental features made on the basis of a correlation between the experimental and calculated spectra are presented in Table 1S of the Supporting Information. It is clear that the experimental features seen in the difference spectrum recorded in acid aqueous solvent are reproduced very well in the calculations and this strongly supports the assignment of the spectrum to 2-BPy-NH^+.

The B3LYP/6-311G** calculations show that attachment of the proton to the pyridine nitrogen atom causes the bond lengths of 2-BPy to change noticeably, especially those in the pyridyl group (a detailed discussion about the structure is given in the Supporting Information). The Raman feature at 1673 cm^{-1} in the experimental spectrum of 2-BPy-NH^+ represents the carbonyl C=O stretching vibration and has a 12 cm^{-1} upshift relative to the corresponding vibration at 1661 cm^{-1} observed in neutral aqueous solvent. This result is consistent with the structure of 2-BPy-NH^+ predicted by DFT calculations in which the C=O bond length is 1.2191 Å, shorter than that of 1.2205 Å in the neutral 2-BPy species. Thus, in MeCN and neutral and basic aqueous solvents, 2-BPy exists in the neutral form whereas in the acidic aqueous solvent 2-BPy-NH^+ is the predominant form.

Femtosecond transient absorption (fs-TA) spectroscopy of 2-BPy in MeCN and aqueous solvents: Figure 3 displays representative fs-TA spectra of 2-BPy in MeCN and neutral aqueous solvents at room temperature after 266 nm photoexcitation. Inspection of Figure 3 shows that the spectra acquired in neat MeCN (A) and in neutral aqueous solvent (B) are similar at short delay times as a broad absorption (λ_{max} = 560 nm) was observed that can be assigned to the

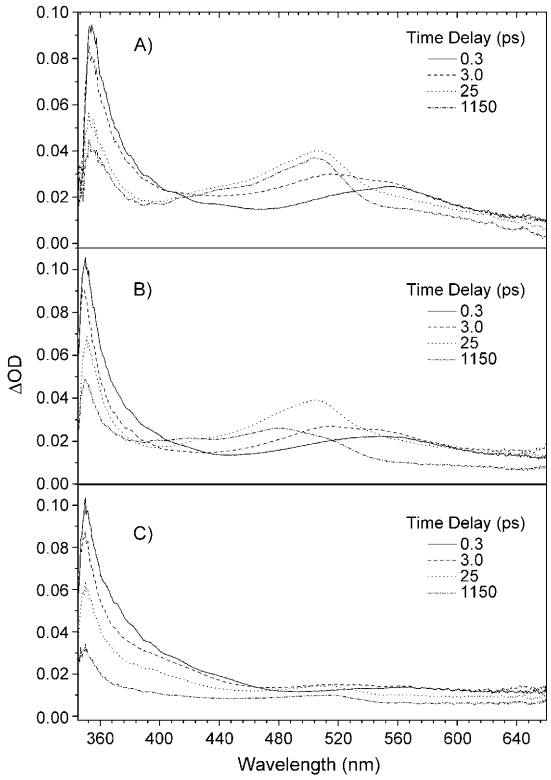

Figure 3. fs-TA spectra of 2-BPy in A) MeCN, B) neutral and C) acidic aqueous solvent recorded with 267 nm excitation.

$S_1 \rightarrow S_n$ transition.[24,38] The initial changes in the spectra have mainly been attributed to $S_1 \rightarrow T_1$ intersystem crossing (ISC), which results in the well-known absorption corresponding to the $T_1 \rightarrow T_n$ transition with a maximum at 505 nm. The formation of the T_1 states was monitored at 505 nm and the results are displayed in Figure 4 together with exponential fittings of the experimental data points. The temporal change of the 505 nm band can be fitted by using a bi-exponential growth function with time constants of $t_1 = (0.48 \pm 0.07)$ (45.3 %) and $t_2 = (6.4 \pm 0.7)$ ps (54.7 %) in MeCN and $t_1 = (0.63 \pm 0.11)$ (56.7 %) and $t_2 = (6.9 \pm 1.5)$ ps (43.3 %) in neutral aqueous solvent. The short growth time is due to the ultrafast internal conversion (IC) of S_n directly to S_1 (S_1 also has an absorption contribution at 505 nm) and the higher value results from the $S_1 \rightarrow T_1$ transition. The $S_1 \rightarrow T_1$ transition time of ≈6 ps is shorter than the ≈10 ps observed for BP[38] and this indicates that the presence of nitrogen in the aromatic ring accelerates the ISC rate of the 2-BPy molecule. Considering the remarkable differences in the polarity and hydrogen-bonding ability of MeCN and water, the similarity of the spectra and dynamics of the two solvent systems suggests there is only a modest influence of these solvent properties on these processes. This result is consistent with the nearly solvent-independent ISC dynamics reported in our previous studies on the benzoin diethyl phosphate molecule system.[39]

However, the spectra recorded in the neutral aqueous solvent at longer delay times display distinctly different fea-

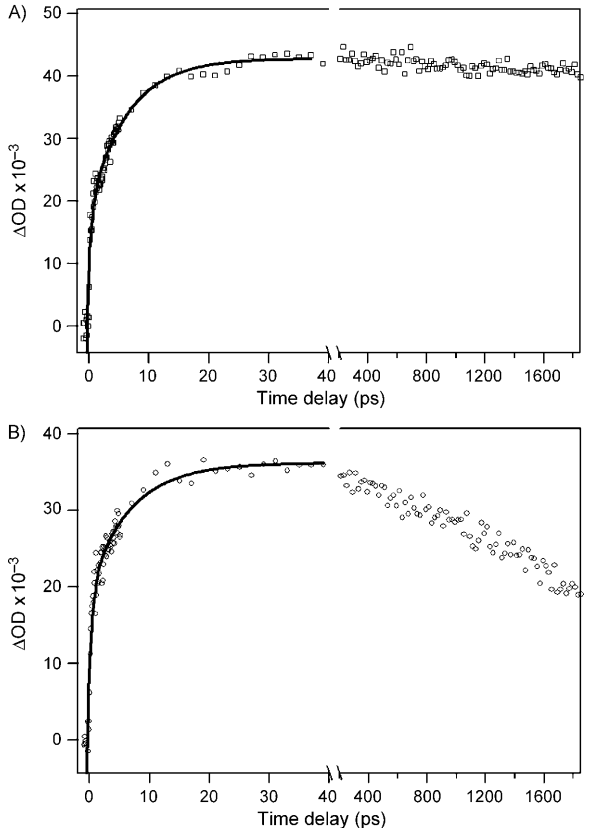

Figure 4. The time-dependence of the transient absorption spectra of 2-BPy in A) MeCN and B) neutral aqueous solvent monitored at 505 nm. The solid lines indicate the fitting of the kinetics to the experimental data points using exponential functions (see text for more detail).

tures to those observed in MeCN. In neat MeCN, the absorption of the triplet 2-BPy persisted up to 1.8 ns, which is the maximum measurement time-delay of our instrument (shown in Figure 4A). However, in the neutral aqueous solvent, the triplet decayed but not completely within 1.8 ns (see Figure 4B) and produces a new species that has a maximum absorbance at 480 nm and a shoulder at 420 nm (see the 1150 ps spectrum, Figure 3B). This result is consistent with a previous observation[16] and indicates that the latter (480 nm absorbing) species should be the cyclisation intermediate, *cis* biradical **2** (see Scheme 1).[16] A similar fs-TA measurement was performed in the basic aqueous solvent and the spectra obtained are shown in Figure S5 in the Supporting Information. The fs-TA spectra recorded in the basic aqueous solvent are almost the same as those recorded in the neutral aqueous solvent.

The absorption spectra (Figure 3C) recorded in the acidic aqueous solvent are significantly different to those recorded in neat MeCN and in the neutral and basic aqueous solvents. The 0.3 ps spectrum displays a long tail beyond 440 nm although with a small absorption band at ≈560 nm. This pattern differs to that of the S_1 state of 2-BPy in MeCN and the neutral aqueous solvent. Because the ground state 2-BPy-NH^+ is the major species in the acidic aqueous solvent, we tentatively attribute the 0.3 ps spectrum to its S_1 state. As the 2-BPy-NH^+ S_1 state decays, a new absorbance band develops at 514 nm as well as a shoulder at 390 nm to the band at 350 nm, as shown in the 25 ps spectrum (Figure 3C). This spectrum closely resembles that of triplet BP-OH^+, which has clear absorption bands at 500, 385 and 320 nm.[24] This result indicates that the triplet 2-BPy-OH^+ is generated and then decays, but not completely within the observable timescale of our instrument. All these results provide further support that the conformation of 2-BPy in acidic aqueous solvent is not the neutral 2-BPy (shown in the above sections) and also implies that the species recorded in the ns-TR^3 spectra in the acidic aqueous solvent (this will be presented in a later section) does not result from the nπ* triplet 2-BPy.

Nanosecond time-resolved resonance Raman (ns-TR^3) spectroscopy and comparison with the results of DFT calculations

ns-TR^3 study in MeCN: Figure 5A displays the transient resonance Raman spectrum of 2-BPy in MeCN obtained at a nominal time delay of 0 ns and an overview of the TR^3 spec-

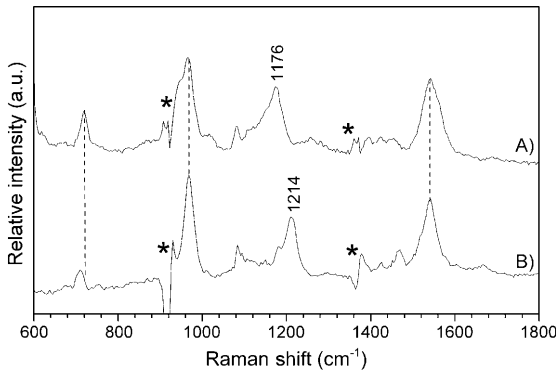

Figure 5. The transient resonance Raman spectrum of A) 2-BPy in MeCN acquired at a nominal 0 ns time delay between the pump and probe pulses is compared with B) the triplet BP spectrum. The two spectra were obtained with 266 nm pump and 319.9 nm probe excitation wavelengths.

tra acquired for 2-BPy in MeCN at a number of different time delays is presented in Figure S1 of the Supporting Information. Only one species was observed after 266 nm laser pulse photolysis of 2-BPy in MeCN. This species was assigned to triplet 2-BPy because it is sensitive to oxygen and its resonance Raman spectrum is very similar to that of triplet BP (see Figure 5B). Examination of Figure 5 shows that the resonance Raman spectrum of the triplet 2-BPy species corresponds well to that of triplet BP with only moderate differences, such as the Raman feature corresponding to a 40 cm^{-1} downshift of the carbonyl C–O stretch from 1214 cm^{-1} in the triplet BP spectrum to 1176 cm^{-1} in the triplet 2-BPy. The tentative vibrational assignments based on DFT calculations of the Raman frequencies predict that

the carbonyl C–O stretching combined with the C–H in-plane bending vibration motion contribute to the vibration frequencies at 1185 and 1162 cm^{-1} for the triplet 2-BPy but only to the frequencies at 1211 cm^{-1} for the triplet BP. Therefore it is not surprising that the substitution of nitrogen in the phenyl group changes the triplet 2-BPy structure significantly compared with that of the triplet BP. For example, the C–O bond in the triplet 2-BPy state is 1.311 Å compared with 1.324 Å in the triplet BP state. Moreover, the orientation of the carbonyl bond with respect to the plane of the phenyl group is 27°, whereas it is only 7° between the carbonyl bond and the plane of the pyridyl group in the triplet 2-BPy. In previous studies the frequency of the C–O stretch mode appears in the 1400–1600 cm^{-1} range for a ππ* dominated triplet state whereas this mode will appear in the 1200–1400 cm^{-1} region for a typical nπ* triplet state.[28,39] As illustrated above, the C–O stretching frequency for the triplet 2-BPy is at 1176 cm^{-1}, which indicates that the triplet 2-BPy has an nπ* dominated configuration, in good agreement with previous reports on the electron-withdrawing effect of the heterocyclic nitrogen atom enhancing the triplet nπ* character of benzoylpyridine.[6,8,13,15,16,18]

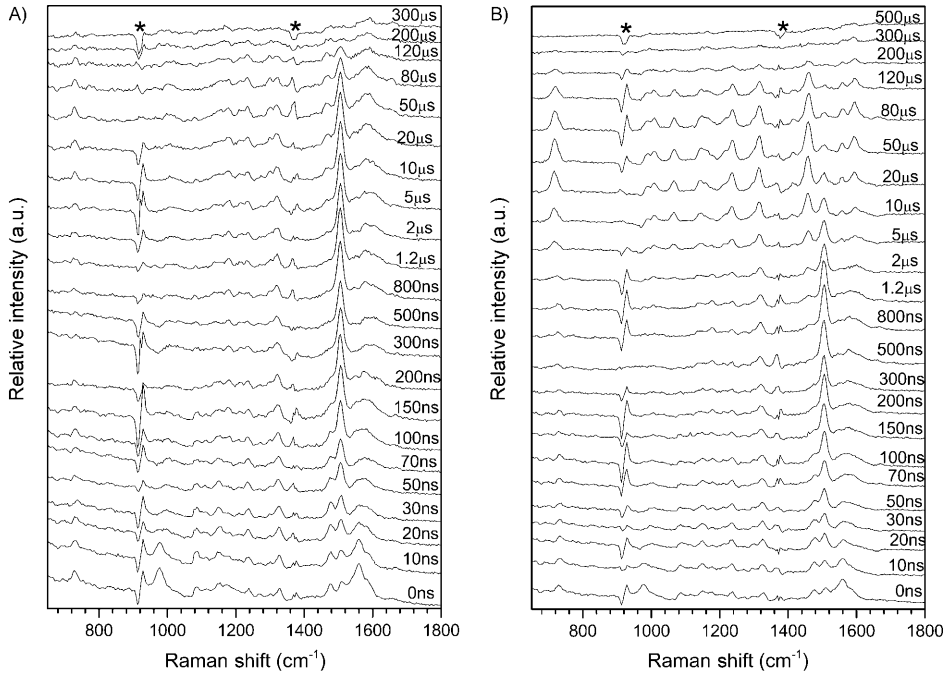

Figure 6. Nanosecond time-resolved resonance Raman spectra of 1.5 mM 2-BPy in A) neutral and B) basic aqueous solvents obtained with a 266 nm pump excitation wavelength and a 309.1 nm probe wavelength at various delay times. The asterisks mark regions that may be affected by subtraction artefacts.

The characteristic Raman band at 1543 cm^{-1} for the triplet 2-BPy was integrated with Lorentzian band shapes and the integrated intensity of this band could be fitted very well by a single-exponential decay function with a time constant of (56 ± 5) ns, as shown in Figure S2 of the Supporting Information. This result is comparable with that for the decay of triplet BP with a time constant of 75 ns in MeCN[28] and also suggests that the triplet 2-BPy is produced with a high quantum yield close to unity due to the small energy gap and strong spin–orbit coupling between the exited singlet and triplet states of 2-BPy.

ns-TR³ study in neutral and basic aqueous solvents: Figure 6 displays representative ns-TR³ spectra of 2-BPy acquired in neutral (A) and basic (B) aqueous solvents with time delays between the 266 nm pump and 309.1 nm probe pulses varying from 0 ns to 300 and 500 μs, respectively. The spectra in Figure 6 show that the UV photolysis of 2-BPy in aqueous solvent produces a very complicated photochemical behaviour that involves several different transient species. At 0 ns, the characteristic bands at 977 and 1557 cm^{-1} are the strongest for triplet 2-BPy, which in neutral and basic aqueous solvents has a lifetime shorter than 20 ns (see the 977 cm^{-1} Raman band in Figure 6) and coexists with another species characterised by Raman bands at 1475 cm^{-1} at short delay times. This result is consistent with the fs-TA observations that the triplet 2-BPy decayed and generated a new species with a maximum absorption at 480 nm in the neutral and basic aqueous solvents. The dynamics of the latter species was obtained by fitting the 1475 cm^{-1} Raman band area with a Lorentzian function and was fitted well by an exponential decay function with time constants of ≈115 and ≈120 ns in the neutral and basic aqueous solvents, respectively. As the 1475 cm^{-1} Raman band decays another new species gradually grows with a strong Raman band at 1506 cm^{-1}. The kinetics of the species associated with the 1506 cm^{-1} band in the neutral aqueous solvent can be obtained by fitting the change in the intensity of the band with exponential growth and decay components. This fitting gives time constants of ≈113 ns, determined for its growth combined with a decay time of ≈76 μs. The correlated time constants for the decay of the 1475 cm^{-1} band (≈115 ns) and the growth of the 1506 cm^{-1} band (≈113 ns) imply that there is a direct transformation of the species associated with the 1475 cm^{-1} band into the species associated with the 1506 cm^{-1} band being produced. However, in the basic aqueous solvent, the areas of the latter were fitted better by using an exponential growth function combined with two exponential decay functions. The time constant observed in the basic aqueous solvent was estimated to be ≈120 ns for its growth and ≈4.1 μs (64%) for a fast decay component and ≈76 μs (36%) for a slow decay component. The slow

decay component closely resembles the behaviour observed in the neutral aqueous solvent in which, under the conditions of observation, no new Raman bands are seen after the 1506 cm^{-1} Raman band disappears, but there is a new species in the basic aqueous solvent that appears and displays clear Raman spectra between 5 and 120 μs, as shown in Figure 6. This new species observed under basic aqueous conditions exhibits a number of Raman bands, namely those at 720, 1234, 1317, 1459, 1564 and 1595 cm^{-1}. The 1459 cm^{-1} band was selected to follow the kinetics of the new species and its area is fitted well by using an exponential growth function with a time constant of ≈15.3 μs and a decay component with a time constant of ≈155 μs. The time dependences of the areas of the Raman bands and the fitted exponential functions, including the estimated time constants mentioned above, are all presented in Figure S3 of the Supporting Information.

Further ns-TR^3 measurements in neutral and basic aqueous solvents using a 309.1 nm probe wavelength were also performed with oxygen-purging (these results are shown in Figure S4 of the Supporting Information). The spectra acquired with oxygen-purging show that the lifetime of the species associated with the 1506 cm^{-1} Raman band is no different to that obtained in the presence of air, as reported above. This suggests that the new species at 1506 cm^{-1} should not have triplet character.

In aqueous solvent, the shorter lifetime of 2-BPy is due to a fast intramolecular photocyclisation with the formation of a pyrrole ring.[4] Previous studies using pico- and nanosecond-resolved laser flash photolysis techniques revealed two different photoreaction pathways (Scheme 1) in aqueous solvent.[16] The *cis* conformation pathway is predominant with the *trans* conformation product **3'** only a minor product in stronger hydrogen-bonding systems such as water.[16] In addition, the *cis* biradical **2** has a lifetime of 450 ns and the *cis* zwitterionic singlet **3** has a lifetime of 600 μs under the experimental conditions used by Favaro and co-workers.[16] These results are consistent with the lifetimes of the new species observed in the TR^3 spectra obtained in the neutral and basic aqueous solvents. Thus, the two new species associated with the 1475 and 1506 cm^{-1} Raman bands observed in the TR^3 experiments are tentatively assigned to the *cis* biradical **2** and the singlet species **3**, respectively.

Figure 7 presents the RR spectra of the *cis* biradical **2** and singlet species **3**. To characterise the biradical **2** (the 1475 cm^{-1} species) clearly, the transient Raman spectrum obtained at 0 ns using a 319.9 nm probe wavelength in neat MeCN was appropriately scaled and subtracted from the spectrum obtained in neutral aqueous solvent under the same experimental conditions. The absence of the predicted carbonyl stretching feature at ≈1700 cm^{-1} for the *cis* biradical **2** (Figure 7A) in the experimental spectrum can probably be accounted for by the resonance Raman enhancement effect on the Raman intensities observed in the experimental spectrum.

The new species associated with the 1459 cm^{-1} Raman band and uniquely observed in the basic aqueous solvent appears after the *cis* singlet **3** decays and its growth rate is much slower (≈15.3 μs) than the decay rate of the *cis* singlet **3** species (≈4.1 μs). A possible mechanism is proposed in Scheme 2 and this new species was tentatively assigned to

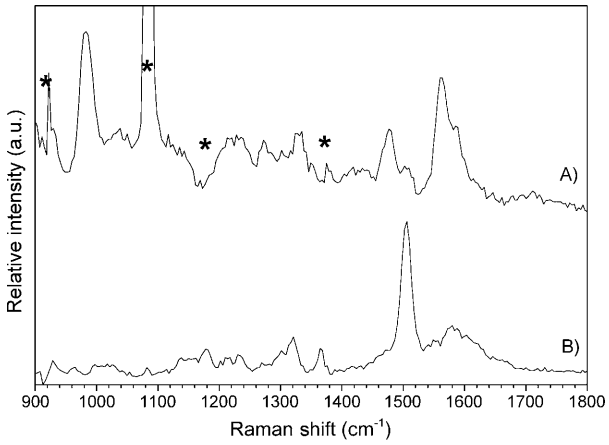

Figure 7. A) RR spectrum for *cis* biradical **2** obtained after 266 nm laser photolysis of 2-BPy in neutral aqueous solvent with a 319.9 nm probe at a delay time of 0 ns after subtraction of an appropriately scaled spectrum obtained in MeCN under the same experimental conditions. B) RR spectrum of *cis* singlet **3** acquired after 266 nm laser photolysis of 2-BPy in neutral aqueous solvent at a time delay of 1.2 μs . The asterisks mark subtraction artefacts.

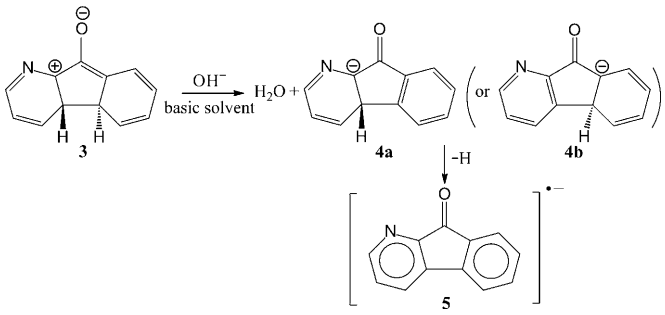

Scheme 2. Possible mechanism for the formation of radical anion **5** in basic aqueous solvent.

the radical anion **5**. A B3LYP/6-311G** DFT calculation was performed to localise the stable geometry of the radical anion **5** and the result shows that radical anion **5** has a near-planar structure with the radical ion delocalised throughout the ring system. Figure 8 allows the DFT-predicted Raman spectrum of radical anion **5** to be compared with the experimental spectrum obtained by using the 50 μs Raman spectrum acquired in the basic aqueous solvent with a 309.1 nm probe wavelength and subtracting the spectrum recorded at a delay time of 200 ns under the same conditions. The detailed comparison and possible vibration mode descriptions for the calculated frequencies are listed in Table 2S of the Supporting Information. The intense Raman bands at 1592 and 1557 cm^{-1} are due to a combination of C=O stretching and C–C and C–N aromatic stretching and the Raman

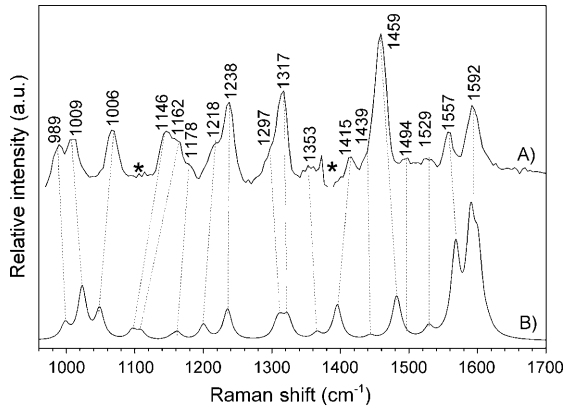

Figure 8. A comparison of the experimental resonance Raman spectra for A) the new species at 1459 cm^{-1} obtained after 266 nm laser photolysis of 2-BPy in the basic aqueous solvent using 309.9 nm as the probe wavelength at a time delay of 50 μs subtracting the scaled spectrum recorded at 200 ns under the same conditions with B) the DFT-predicted normal Raman spectrum for the radical anion **5**. The asterisks mark regions that may be affected by subtraction artefacts. Dashed lines display the correlation between the experimental and calculated Raman bands.

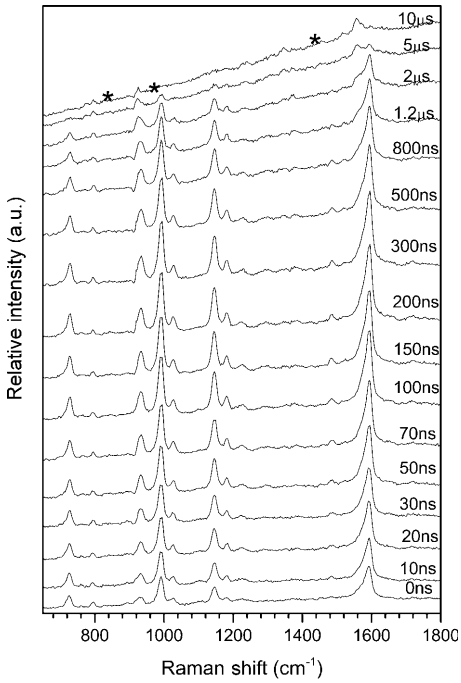

Figure 9. ns-TR^3 spectra of 1.5 mM 2-BPy in acidic aqueous solvent obtained with a 266 nm pump excitation wavelength and a 354.7 nm probe wavelength at various delay times. The asterisks mark regions that may be affected by subtraction artefacts.

bands at 1529, 1494 and 1459 cm^{-1} arise from the C–C and C–N aromatic stretching. The other Raman bands observed in Figure 8 are mainly attributed to the C–H bending in the ring plane. Examination of the spectra in Figure 8 and Table 2S show that the experimental features seen in the ns-TR^3 spectra are reproduced reasonably well by calculations with an average difference frequency of only 12 cm^{-1} for 18 vibration frequencies. This result further supports the assignment of the species formed after a longer time in basic aqueous solvent to the radical anion **5** and also provides further evidence for the assignment of transient species **2** and **3**, which proves the *cis* photocyclisation pathways are more likely in neutral/basic solvents.

TD-DFT calculations found that the anion **4a** or **4b** has a very weak transition at around 309.9 nm, which was used here to excite the molecular system (the details of the TD-DFT calculations are listed in Table 3S of the Supporting Information). Therefore it is possible that the anion **4a** or **4b** cannot be observed under the experimental conditions used because it has a weak oscillator for the transition that could enhance its resonance at the probe wavelength used in the experiments.

ns-TR^3 study in acidic aqueous solvent and assignment of the observed species and possible reactions of 2-BPy after short delay times: Figure 9 displays representative ns-TR^3 spectra of 2-BPy in acidic aqueous solvent acquired with 266 nm pump and 354.7 nm probe wavelengths at various delay times from 0 ns to 10 μs. Under acidic aqueous solvent conditions, the TR^3 results are distinctly different to those obtained in neutral and basic solvent conditions. In the acidic aqueous solvent only one species can be observed on the nano- to microsecond timescale. The integrated areas for the 1594 cm^{-1} Raman band observed in the TR^3 spectra in Figure 9 were plotted as a function of delay time and the data points were fitted by a bi-exponential function with a growth time constant of 54 ns and a decay time constant of 1850 ns (see Figure S6 of the Supporting Information). The same ns-TR^3 experiments were also performed with oxygen-purging (the results are shown in Figure S7) and the lifetime of this species showed a significant decrease compared with that obtained in the presence of air. This result indicates that the species observed in acidic aqueous solvent is likely to have triplet character.

DFT computations were performed to study the photocyclisation of 2-BPy in acidic aqueous solvent.[40] It was suggested that among the eight investigated possible cyclisation reaction pathways, the attack of the nitrogen atom of 2-BPy-OH^+ (Scheme 3) has the lowest free-energy barrier (3.4 kcal mol^{-1}). These computational results also showed this reaction to have the lowest activation free-energy barrier and the biggest negative exothermic energy, which means that the cyclisation reaction involving the attachment of the nitrogen atom in 2-BPy-OH^+ is much more kinetically and

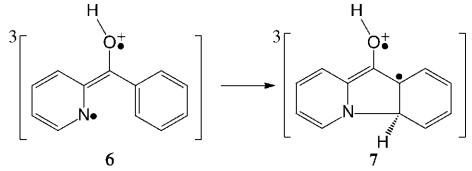

Scheme 3. The lowest free-energy barrier reaction pathway involving the attack of the nitrogen atom of 2-BPy-OH^+.

thermodynamically favourable. On the basis of the high reactivity of the triplet 2-BPy-OH$^+$ in the photocyclisation reaction, the unique species observed in the TR^3 experiments in acidic aqueous solvent was tentatively assigned to the triplet tricyclic cation species **7** in Scheme 3. To verify this assignment, DFT calculations were performed to predict the Raman frequencies of the tricyclic cation **7** and the results compared with the experimental spectrum. Figure 10 presents a comparison of the experimental TR^3 spectrum obtained at 70 ns under acidic aqueous conditions (see Figure 9) with the UB3LYP/6-311G** DFT-calculated normal Raman spectrum of the triplet-state tricyclic cation **7**. Inspection of Figure 10 reveals that the calculated normal Raman spectrum for the triplet state of the tricyclic cation **7** exhibits reasonable agreement with the experimental TR^3 spectrum for the species shown in Figure 9. Ten strong Raman bands were observed at 726, 935, 994, 1027, 1149, 1181, 1225, 1487, 1564 and 1593 cm^{-1}, most of which are due to vibrations associated with ring C–C or C–N stretching and C–H bending motions. The 1593, 1564 and 1487 cm^{-1} Raman bands are mainly due to ring C–C and C–N stretching vibrational modes, the 1225, 1181, 1149, 1027 and 994 cm^{-1} Raman bands are from C–H bending modes and the 935 and 726 cm^{-1} Raman features are attributed to the ring deformation modes. The spectra shown in Figure 10 display moderate differences in their relative Raman intensity patterns and this is likely accounted for by resonant enhancement of the experimental spectrum whereas the calculated spectrum is a non-resonant Raman spectrum. All these results strongly support assignment of the experimental spectra in Figures 9 and 10 to the triplet tricyclic cation **7**.

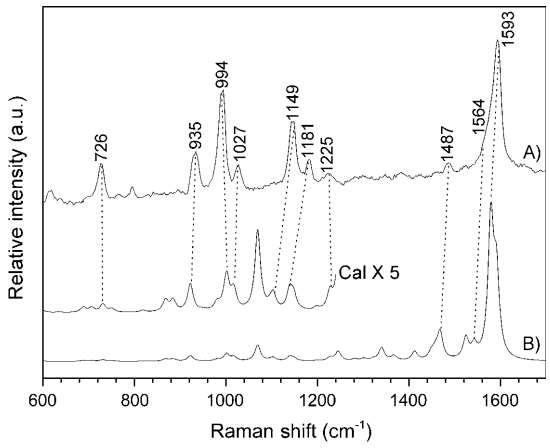

Figure 10. A comparison of A) the experimental resonance Raman spectra of 2-BPy in acidic aqueous solvent at a 70 ns delay time and B) the DFT-predicted normal Raman spectra of the triplet tricyclic cation **7**. The inset displays an enlarged view of the calculated spectrum in the 600–1300 cm^{-1} region for easier comparison of the less intense Raman bands. Dotted lines display the correlation between the experimental and calculated Raman bands.

The RR spectrum of 2-BPy recorded in acidic aqueous solvent with 309.9 nm excitation reveals (at least in the mixed aqueous solvent containing 0.05 M $HClO_4$ examined here and shown in Figure 2E) that most of the 2-BPy is protonated and exists mainly in the ground state 2-BPy-NH$^+$ form. This result is consistent with the higher value of pK_a of the pyridine nitrogen atom relative to the carbonyl oxygen atom, which remains negligibly protonated even in a 5.8 M $HClO_4$ solution.[34] The fs-TA spectrum obtained immediately after 267 nm photolysis of 2-BPy in an acidic aqueous solvent after a short time (see the 0.3 ps spectrum in Figure 3C) shows significant differences to the analogous spectrum recorded in the neutral aqueous solvent and this provides further confirmation that the precursors of the photoreaction are likely different in the acidic and neutral aqueous solvents. Both the neutral 2-BPy ground state and its excited states, including S_1 and T_1, exhibit similar electron configurations to those of the corresponding states of BP[16] and this was also verified by the UV/Vis steady-state absorption and fs-TA measurements reported in the previous sections. Therefore the fs-TA spectra recorded at 0.3 and 25 ps in acidic aqueous solvent were assigned to the 2-BPy-NH$^+$ lowest singlet (S_1) state and the 2-BPy-OH$^+$ triplet (T_1) due to their resemblance to the spectra of the S_1 state of neutral 2-BPy and the BP-OH$^+$ species.[24,38]

The 2-BPy-NH$^+$ S_1 state evolves into the 2-BPy-OH$^+$ T_1 by excited-state proton transfer (ESPT), pyridyl group rotation and intersystem crossing (ISC) with the aid of water, as shown in Scheme 4. From our current fs-TA measurements it is hard to identify each process explicitly, but our results suggest all of these processes occur within several tens of picoseconds or even much faster for some of the processes. This result is consistent with a previous study in which it was found that the ESPT process can occur on the timescale of 150 fs to 250 ps in a hydrogen-bonded acid–base complex[41] and in encounter pairs formed by the diffusion of uncomplexed photoacid and -base molecules,[42,43] respectively. The ESPT process here appears to prefer to occur in the lowest singlet states (S_1) rather than in the lowest triplet states (T_1) as a result of the triplet-state energies of the reactions predicted by the DFT calculations. The results of the

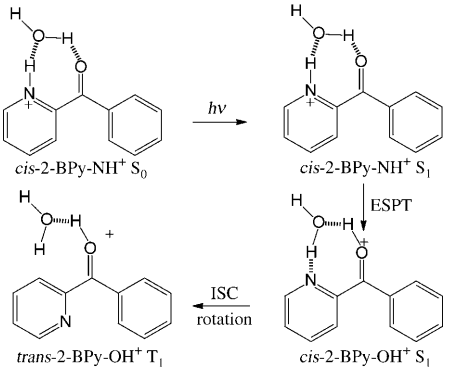

Scheme 4. Possible mechanism for the reaction of 2-BPy in acidic aqueous solvent after a short reaction time.

DFT calculations show that the *cis*-2-BPy-OH^+ triplet T_1 has an energy ≈ 12 kcal mol^{-1} higher than that of the *cis*-2-BPy-NH^+ triplet T_1 and this means there is a reaction barrier of more than 12 kcal mol^{-1} for the direct conversion of *cis*-2-BPy-NH^+ T_1 into *cis*-2-BPy-OH^+ T_1. The presence of such a barrier is not consistent with our observation that all of the processes involved in the evolution of 2-BPy-NH^+ S_1 to 2-BPy-OH^+ T_1 occur within several tens of picoseconds.

Comparison of the triplet 2-BPy and BP species: The triplet 2-BPy observed in the fs-TA and ns-TR^3 measurements displays an nπ* character similar to the triplet BP. In addition, substitution of the heterocyclic nitrogen atom leads to a slight change in the triplet geometry as a result of differences in the carbonyl bond length and in the orientation between the pyridyl and phenyl groups and these changes are reflected in the vibrational Raman frequencies seen at 1176 cm^{-1} for the triplet 2-BPy and 1214 cm^{-1} for the triplet BP in their transient Raman spectra (see Figure 5). This is consistent with previous reports about the electron-withdrawing effect of the heterocyclic nitrogen enhancing the benzoylpyridine triplet nπ* character.[6,8,13,15,16,18] In neutral aqueous solvent, the triplet BP still exhibits nπ* character and abstraction of hydrogen from water to produce a ketyl radical is the major reaction pathway.[37] However, the triplet 2-BPy in neutral aqueous solvent undergoes a fast cyclisation reaction, which suggests the triplet has some ππ* character and hence loses some of its capacity for hydrogen abstraction.[16] This transformation of the electronic configuration for the triplet 2-BPy is likely a result of hydrogen-bonding with water molecules.[16]

Triplet BP in the acidic aqueous solvent is protonated very quickly to form the triplet BP-OH^+, which will be attacked by water at the *ortho* or *meta* position to produce hydration intermediates and photoproducts.[24,37] The fs-TA and ns-TR^3 experimental measurements and the DFT results[40] imply that the triplet 2-BPy-OH^+ is also generated in the acidic aqueous solvent during the UV laser-induced photoreaction. But this triplet 2-BPy-OH^+ results from the corresponding triplet 2-BPy-NH^+ precursor by ESPT, ISC and pyridyl group rotation processes and all of these processes can occur with the assistance of water molecules.

Different photocyclisation reactions in neutral/basic and acidic aqueous solvents: In both neutral/basic and acidic aqueous solvents, cyclisation reactions take place to produce cyclisation intermediates and products, but the photocyclisation reactions in these two different types of aqueous solvents occur by very different mechanisms. In the neutral/basic aqueous solvent the photocyclisation reaction involves the carbon atom of the pyridyl group whereas in acidic aqueous solvent the reaction involves the nitrogen atom in the pyridyl group with the lone pair involved in the mechanism (see Scheme 5). The results of fs-TA experiments have revealed that the ISC rate constant for the conversion of S_1 into T_1 for neutral 2-BPy is ≈ 6 ps in neat MeCN and neutral/basic aqueous solvents with the nπ* triplet 2-BPy the precursor of the photocyclisation step in neutral and basic aqueous solvents. The ns-TR^3 spectra recorded in neutral aqueous solvent provide the first vibrational spectral characterisation of the *cis* biradical 2 and *cis* singlet zwitterionic species 3.[16] In the basic aqueous solvent, as the *cis* singlet zwitterionic species 3 decays a new species grows, which, with the help of a comparison with the DFT-predicted Raman spectrum, was tentatively assigned to the radical anion 5. However, in the acidic aqueous solvent the ground state 2-BPy-NH^+ prevails and after laser photolysis the S_1 of 2-BPy-NH^+ is generated, which evolves into the T_1 of 2-BPy-OH^+. The photocyclisation step then takes place through the pyridyl nitrogen atom to produce the triplet tricyclic cation 7. This different behaviour is mainly caused by

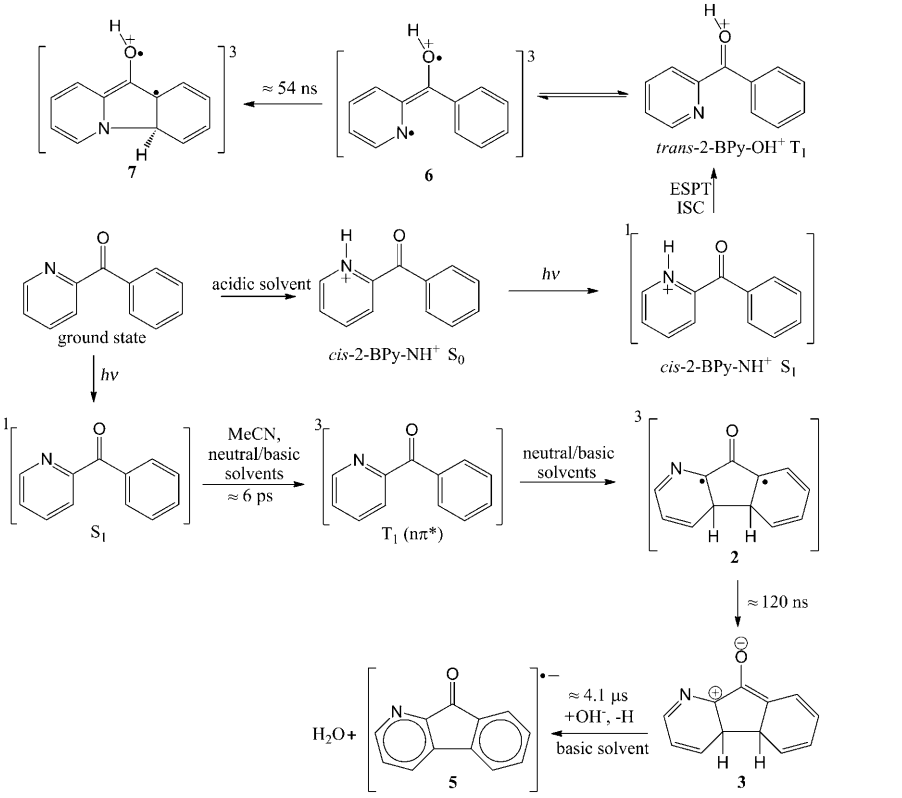

Scheme 5. Summary of the transient species observed after UV laser photolysis of 2-BPy in aqueous solvents.

the different conformations of the precursors and the effect of hydrogen-bonding with the solvent. B3LYP/6-311G** calculations on the neutral form of the 2-BPy ground-state singlet predicts that the *cis* form has an energy 4.4 kcal mol^{-1} higher than the *trans* form in the gas phase whereas in the case of the pyridine nitrogen-protonated 2-BPy cation, the *cis* form has an energy 4 kcal mol^{-1} lower than the *trans* form. Considering the high hydrogen-bonding ability of water, the aqueous solvent would stabilise the *cis* neutral 2-BPy more than its *trans* form, hence the *cis* neutral 2-BPy could prevail in the neutral/basic aqueous solvent and this agrees well with the *cis* product being the major product detected during the photoreaction.[16] However, in the acidic aqueous solvent, the ground state *cis* 2-BPy-NH$^+$ is the predominant species and will convert very quickly into the triplet 2-BPy-OH$^+$ by ESPT and ISC processes after laser photolysis. Moreover, the *trans* triplet 2-BPy-OH$^+$ is predicted to be more stable ($\approx$1.4 kcal mol^{-1}) than its corresponding *cis* form. The observation of triplet 2-BPy-OH$^+$ is in agreement with the DFT calculations that the cyclisation from the *trans* triplet has the lowest-energy barrier among eight possible photocylisation pathways.[40]

The 266 nm laser was used to irradiate 2-BPy in neutral, basic and acidic aqueous solvents at room temperature to gain information on the photocyclisation products of 2-BPy in aqueous solvents. The time course of the 2-BPy spectrum upon irradiation in aqueous solvents is shown in Figure S8 of the Supporting Information. The behaviour of 2-BPy in neutral aqueous solvent is very similar to that reported by Favaro and co-workers[16] and the main product **10** is formed. In basic aqueous conditions, although 2-BPy (λ_{max} = 260 nm) is consumed, only one band with a maximum at around 220 nm grows, which is significantly different to the corresponding experiment in neutral solvent. This result is consistent with our observations in ns-TR^3 experiments that the zwitterion **3** is further alkalinised to generate the radical anion **5**. In the acidic solvent it is also clear that the photoproducts are different to those produced in the neutral/basic solvents. Irradiation of 2-BPy in an air-saturated aqueous solution with UV light in the absence of a donor causes complicated photochemical reactions. Several products were detected when 313 nm was used to excite the 2-BPy sample in aqueous solution but only product **10** was mentioned in a previous study.[35] In this work we aimed to utilise fs-TA and ns-TR^3 experiments to gain an understanding of the mechanism of the fast photocyclisation reaction of 2-benzoylpyridine in aqueous solvent, however, due to a lack of clear characteristic absorption bands, we cannot determine the structures of these photoproducts at this time in acidic solvent as has been done in neutral and basic solutions.

Conclusion

A combined fs-TA and ns-TR^3 spectroscopic investigation of the photoreactions of 2-BPy in MeCN and neutral, basic and acidic aqueous solvents has been described and observed transient species are shown in Scheme 5. The *cis* biradical **2** and *cis* singlet zwitterionic species **3** have been characterised for the first time by time-resolved vibrational spectroscopy. A new species generated in the basic solvent after the decay of the zwitterion **3** was observed for the first time and, in conjunction with results from DFT calculations, this new species was identified as the radical anion **5**, which provides further evidence for the controversial mechanism that in a hydrogen-bonding solvent the photocyclisation reaction should take place at the carbon atom in the pyridyl group. The fs-TA experiments revealed the nπ* triplet 2-BPy to be the precursor of the photocyclisation reaction in neutral and basic aqueous solvents whereas in acidic aqueous solvent the S_1 species 2-BPy-NH$^+$ and T_1 species 2-BPy-OH$^+$ were generated after photolysis of ground state 2-BPy-NH$^+$. The identification and characterisation of triplet tricyclic cation **7** provide new insights into the reaction mechanism of the photocyclisation of 2-BPy in an acidic aqueous solvent, which has never been studied over such a broad timescale from femtosecond to microsecond. The fs-TA and ns-TR^3 spectral and dynamic data combined with DFT calculations presented here provide essential information for achieving a comprehensive consensus of the molecular origin of the photocyclisation reaction mechanism for 2-BPy in aqueous solutions.

Experimental Section

Materials: Samples of BP and 2-BPy were obtained from Aldrich (with >99% purity), sodium hydroxide from UNI-Chem (with >96% purity) and perchloric acid from A.C.S. ($HClO_4$, approx 70%) were used as received to prepare the sample solutions used in the experiments. Spectroscopic-grade MeCN and deionised water were used as solvents in the experiments presented in this work. Sample solutions were prepared in neat MeCN, neutral aqueous (H_2O/MeCN, 1:1 by volume), basic aqueous (H_2O/MeCN, 1:1 by volume containing 0.05 M NaOH) and acidic aqueous (H_2O:MeCN, 1:1 by volume containing 0.05 M $HClO_4$) solvents respectively.

fs-TA experiments: fs-TA measurements were performed with a femtosecond Ti:Sapphire regenerative amplifier laser system. For the experiments presented here, the sample solution was excited by a 267 nm pump beam (the third harmonic of the fundamental 800 nm from the regenerative amplifier) and probed by a white-light continuum produced from a translating CaF_2 plate pumped by fundamental laser pulses (800 nm). The pump and probe laser beam spot sizes on the sample were about 120 and 60 μm, respectively. The probe beam was focused into a monochromator and detected with a photodiode array. The time delay between the pump and probe pulse was controlled by an optical delay line and the time resolution of the measurement was ≈200 fs. The TA experiments were performed by using a wire-guided flowing liquid jet (≈100 μm thick film) with a sample concentration of ≈10 mM.

ns-TR^3 experiments: ns-TR^3 measurements were carried out with an experimental apparatus described previously.[28,31,33,39] The pump wavelength of 266 nm was supplied by the fourth harmonic of a Spectra Physics LAB-170-10 Nd:YAG Q-switched laser and the 319.9 nm probe wavelength came from the second Stokes line of a hydrogen Raman-shifted line pumped by the second harmonic (532 nm) from the second Nd:YAG laser (Spectra Physics GCR-150–10) and the other 354.7 and 309.1 nm probe wavelengths were produced from the third harmonic and the first anti-Stokes line of a hydrogen Raman-shifted line pumped by the third harmonic from the same second Nd:YAG laser. The time delay between

the pump and probe beams was controlled electronically by a pulse delay generator and was monitored with a photodiode and a 500 MHz oscilloscope. The time resolution of our experiments was ≈10 ns. The energies of the pump and the probe pulses were in the 2.5–3.5 mJ range with a repetition rate of 10 Hz. A near-collinear geometry was employed to focus the pump and probe beam onto a flowing liquid stream of the sample and the Raman scattering was collected in a backscattering configuration and detected by a CCD detector cooled with liquid nitrogen. The Raman signal was acquired by CCD for 30–60 s before being fed into an interfaced PC computer and approximately 10 to 20 these readouts were accumulated to produce a resonance Raman spectrum. The spectra presented in this work were produced by subtraction of an appropriately scaled probe-before-pump spectrum from the corresponding pump-probe spectrum. MeCN Raman bands were used to calibrate the TR^3 spectra with an estimated accuracy of $\pm 5\ cm^{-1}$ in absolute frequency and a Lorentzian function was used to integrate the relevant Raman bands in the TR^3 spectra so as to determine their areas and to extract the decay and growth kinetics of the species observed in the experiments.

DFT calculations: The optimised geometries, vibrational modes and frequencies for the ground and triplet states of the different species formed in the photoreaction schemes were obtained from (U)B3LYP density functional theory (DFT) calculations employing a 6-311G** basis set. No imaginary frequency modes were observed at any of the optimised structures shown. All of the calculations were performed by using the Gaussian 03 program suite.[44]

Acknowledgements

This work was supported by a grant from the Research Grants Council of Hong Kong (HKU 7035/08P and HKU 1/01C), the award of a Croucher Foundation Senior Research Fellowship (2006-07) from the Croucher Foundation and an Outstanding Researcher Award (2006) from the University of Hong Kong to D.L.P. Work performed at the University of Rochester was supported by start-up funding to D.W.M.

[1] G. S. Hammond, W. P. Baker, W. M. Moore, *J. Am. Chem. Soc.* **1961**, *83*, 2795–2799.
[2] W. M. Moore, G. S. Hammond, R. P. Foss, *J. Am. Chem. Soc.* **1961**, *83*, 2789–2794.
[3] F. L. Minn, C. L. Trichilo, C. R. Hurt, N. Filipescu, *J. Am. Chem. Soc.* **1970**, *92*, 3600–3610.
[4] C. R. Hurt, N. Filipescu, *J. Am. Chem. Soc.* **1972**, *94*, 3649–3651.
[5] G. Favaro, *J. Chem. Soc., Perkin Trans. 2* **1976**, 869–874.
[6] G. Favaro, *J. PhotoChem.* **1986**, *33*, 261–265.
[7] G. Favaro, F. Masetti, A. Romani, *Spectrochim. Acta, Part A* **1989**, *45*, 339–346.
[8] F. Elisei, G. Favaro, A. Romani, *Chem. Phys.* **1990**, *144*, 107–115.
[9] G. Favaro, F. Masetti, A. Romani, *J. Photochem. Photobiol., A* **1990**, *53*, 41–49.
[10] F. Elisei, G. Favaro, H. Goerner, *J. Photochem. Photobiol. A* **1991**, *59*, 243–253.
[11] N. J. Turro, *Modern Molecular Photochemistry*, University Science Books, Mill Valley, **1991**.
[12] A. Romani, F. Elisei, F. Masetti, G. Favaro, *J. Chem. Soc. Faraday Trans.* **1992**, *88*, 2147–2154.
[13] A. Albini, P. Bortolus, E. Fasani, S. Monti, F. Negri, G. Orlandi, *J. Chem. Soc., Perkin Trans. 2* **1993**, 691–695.
[14] F. Elisei, G. Favaro, F. Ortica, *J. Chem. Soc. Faraday Trans.* **1994**, *90*, 279–285.
[15] F. Ortica, F. Elisei, G. Favaro, *J. Chem. Soc. Faraday Trans.* **1995**, *91*, 3405–3413.
[16] P. Bortolus, F. Elisei, G. Favaro, S. Minti, F. Ortica, *J. Chem. Soc. Faraday Trans.* **1996**, *92*, 1841–1851.
[17] G. Balakrishnan, S. Umapathy, *Chem. Phys. Lett.* **1997**, *270*, 557–563.
[18] F. Bosca, M. A. Miranda, *J. Photochem. Photobiol. B* **1998**, *43*, 1–26.
[19] A. Romani, F. Ortica, G. Favaro, *Chem. Phys.* **1998**, *237*, 413–424.
[20] F. Ortica, F. Elisei, G. Favaro, *J. Phys. Org. Chem.* **1999**, *12*, 31–38.
[21] R. Anandhi, S. Umapathy, *J. Raman Spectrosc.* **2000**, *31*, 331–338.
[22] G. Balakrishnan, P. Mohandas, S. Umapathy, *J. Phys. Chem. A* **2001**, *105*, 7778–7789.
[23] G. Favaro, F. Ortica, A. Romani, *Chem. Phys.* **2002**, *280*, 163–175.
[24] M. Ramseier, P. Senn, J. Wirz, *J. Phys. Chem. A* **2003**, *107*, 3305–3315.
[25] X. C. Cai, M. Sakamoto, M. Fujitsuka, T. Majima, *Chem. Eur. J.* **2005**, *11*, 6471–6477.
[26] M. Sakamoto, X. Cai, M. Fujitsuka, T. Majima, *J. Phys. Chem. A* **2005**, *109*, 6830–6835.
[27] N. Basaric, D. Mitchell, P. Wan, *Can. J. Chem.* **2007**, *85*, 561–571.
[28] Y. Du, C. S. Ma, W. M. Kwok, J. Xue, D. L. Phillips, *J. Org. Chem.* **2007**, *72*, 7148–7156.
[29] H. Görner, *J. Photochem. Photobiol A* **2007**, *187*, 105–112.
[30] J. F. Ireland, P. A. H. Wyatt, *J. Chem. Soc. Faraday Trans. 1* **1973**, *69*, 161–168.
[31] Y. Du, J. Xue, C. S. Ma, W. M. Kwok, D. L. Phillips, *J. Raman Spectrosc.* **2008**, *39*, 503–514.
[32] H. Görner, *Chem. Phys.* **2008**, *344*, 264–272.
[33] J. Xue, P. Y. Chan, Y. Du, Z. Guo, C. W. Y. Chung, P. H. Toy, D. L. Phillips, *J. Phys. Chem. A* **2007**, *111*, 12676–12684.
[34] A. J. Kresge, H. J. Chen, G. L. Capen, M. F. Powell, *Can. J. Chem.* **1983**, *61*, 249–256.
[35] H. Görner, *J. Photochem. Photobiol. A* **2009**, *208*, 141–146.
[36] M. D. Li, Y. Du, C. S. Yeung, D. L. Phillips, *J. Phys. Chem. A* **2009**, *113*, 12215–12224.
[37] Y. Du, J. Xue, M. D. Li, D. L. Phillips, *J. Phys. Chem. A* **2009**, *113*, 3344–3352.
[38] B. K. Shah, M. A. J. Rodgers, D. C. Neckers, *J. Phys. Chem. A* **2004**, *108*, 6087–6089.
[39] C. S. Ma, Y. Du, W. M. Kwok, D. L. Phillips, *Chem. Eur. J.* **2007**, *13*, 2290–2305.
[40] X. G. Guan, Y. Du, J. D. Xue, D. L. Phillips, *J. Phys. Chem. A* **2009**, *113*, 1999–2003.
[41] T. Elsaesser, *Ultrafast Hydrogen Bonding Dynamics and Proton Transfer Processes in the Condensed Phase* (Eds.: T. Elsaesser, H. J. Bakker), Kluwer, Dordrecht, **2002**, pp. 119–153.
[42] M. Rini, B. Z. Magnes, E. Pines, E. T. J. Nibbering, *Science* **2003**, *301*, 349–352.
[43] O. F. Mohammed, D. Pines, J. Dreyer, E. Pines, E. T. J. Nibbering, *Science* **2005**, *310*, 83–86.
[44] Gaussian 98 revision A.7 and Gaussian 03 revision B.05, M. J. Frisch, G. W. Schlegel, H. B. Scuseria, G. E. Robb, M. A. Cheeseman, J. R. Zakrzewski, J. A. Montgomery, Jr., R. E. Stratmann, J. C. Burant, S. Dapprich, J. M. Millam, A. D. Daniels, K. N. Kudin, M. C. Strain, O. Farkas, J. Tomasi, V. Barone, M. Cossi, R. Cammi, B. Mennucci, C. Pomelli, C. Adamo, S. Clifford, J. Ochterski, G. A. Petersson, P. Y. Ayala, Q. Cui, K. Morokuma, D. K. Malick, A. D. Rabuck, K. Raghavachari, J. B. Foresman, J. Cioslowski, J. V. Ortiz, A. G. Baboul, B. B. Stefanov, G. Liu, A. Liashenko, P. Piskorz, I. Komaromi, R. Gomperts, R. L. Martin, D. J. Fox, T. Keith, M. A. Al-Laham, C. Y. Peng, A. Nanayakkara, C. Gonzalez, M. Challacombe, P. M. W. Gill, B. Johnson, W. Chen, M. W. Wong, J. L. Andres, C. Gonzalez, M. Head-Gordon, E. S. Replogle, J. A. Pople, Gaussian Inc., Pittsburgh PA, **2003**.

Received: November 19, 2009
Published online: April 30, 2010

